Journal of Applied Polymer Science

Surface Treatment of Cellulose Fibers with Methylmethacrylate for Enhanced Properties of *in situ* Polymerized PMMA/Cellulose Composites

Moloy Banerjee,[1] Sunanda Sain,[1] Anirudhha Mukhopadhyay,[2] Suparna Sengupta,[3] Tanusree Kar,[4] Dipa Ray[1]

[1]Department of Polymer Science and Technology, University of Calcutta, Kolkata 700009, India
[2]Department of Environmental Science, University of Calcutta, Kolkata 700019, India
[3]Department of Basic Science, Humanities and Social Sciences, Calcutta Institute of Engineering and Management, Tollygunge, Kolkata 700040, India
[4]Department of Materials Science, Indian Association for the Cultivation of Science, Kolkata 700032, India
Correspondence to: D. Ray (E-mail: roy.dipa@gmail.com)

ABSTRACT: Cellulose micro/nanofibers (CNF), prepared from jute fibers were surface treated with methyl methacrylate (MMA) for better dispersion into poly methyl methacrylate (PMMA) matrix. PMMA/cellulose composites were prepared by *in situ* suspension polymerization technique. The surface treatment of CNF was confirmed by Fourier transform infrared spectroscopy (FTIR) and Nuclear magnetic resonance (NMR) analysis. MMA-treated cellulose micro/nanofibers (MCNF) demonstrated improved affinity and dispersion in MMA monomer as well as in the PMMA/cellulose composites. Thermal properties of the cellulose composites were analyzed by differential scanning calorimetry (DSC) and thermogravimetric analysis (TGA). The glass transition temperature (T_g) of PMMA increased by nearly 19°C in the *in situ* cellulose composites compared to that of unreinforced PMMA as indicated by DSC. TGA showed increased thermal stability of the cellulose composites. Enhanced tensile properties as well as significantly lower moisture uptake were observed in the *in situ* prepared PMMA/cellulose composites. © 2013 Wiley Periodicals, Inc. J. Appl. Polym. Sci. **2014**, *131*, 39808.

KEYWORDS: fibers; thermogravimetric analysis (TGA); mechanical properties

Received 13 March 2013; accepted 1 August 2013
DOI: 10.1002/app.39808

INTRODUCTION

Polymer composites are of increasing interest now-a-days as lighter, tougher, energy efficient engineering materials with enhanced thermal and mechanical properties. Extensive work has been done to enhance the performance of polymers by reinforcing with different nanofillers like nanoclays, graphite nanoplatelets, carbon nanotubes, and inorganic nanoparticles. But now it is of extreme interest to incorporate green, renewable, inexpensive cellulosic nanofillers into polymer matrices to develop sustainable materials which meet up the recent demand of lightweight composites with high specific strength and modulus. O'sullivan *et al.*[1] mentioned that nanocellulose shows great potential for application as green nano reinforcing material because it is abundant, renewable and can be made multifunctional. The compatibility of nanocellulose with conventional thermoplastics is a well-known problem because of its polar nature. Another drawback of cellulosic fillers is their poor moisture resistance property. Various treatments are being evaluated to decrease or remove moisture from the nanocellulose with a goal of maintaining the nano scale dimensions of the fibrils. Surface modification of cellulose was attempted by Dankovich *et al.*[2] with plant triglycerides (soybean, rapeseed, olive, and coconut oils). Liu *et al.* [3] showed that the reaction of ultrahigh surface-area cellulose fibers with methacrylate chloride (MACl) produced activated surfaces without altering the fiber morphology. Heterogeneous modification of cellulose with isocyanates bearing an alkenyl function in a non-swelling medium introduced a small but significant number of polymerizable moieties at the surface of the cellulose.[4] Chemical modification of cellulose fibers with glycidyl methacrylate was done.[5] Chemical modification of cellulose with succinic anhydride in ionic liquid with or without catalysts was also done.[6] Catalyst free conversion of alkali cellulose to carboxymethyl cellulose was reported.[7] Various modifications with silane coupling agents were also reported. Physical methods of modifications like low temperature plasma treatment, and corona discharge are of great interest in relation to the improvement in functional properties of vegetable fibers.[8]

Among various synthetic polymers, PMMA is a very important one, which, by virtue of its transparency and low cost, finds wide applications in different areas. Many attempts have been made to enhance the performance of PMMA by reinforcing with different micro or nano-fillers by effective techniques. However, very limited research has been reported on using nanocellulose as reinforcing material for PMMA. PMMA-layered silicate nanocomposites were prepared by *in situ* polymerization method.[9] PMMA nanocomposites with montmorillonite (MMT)[10] and some inorganic clay[11] were reported by some researchers. PMMA showed markedly improved properties in these nanocomposites. *In situ* polymerization technique can be a very effective route for making PMMA/cellulose nanocomposites, but there are very few reports on this. Stable aqueous nanocomposite dispersions based on cellulose whiskers and acrylate latex via mini emulsion polymerization was reported in a recent study.[12] There is one report of preparing PMMA-cellulose nanocomposites by *ex situ* dispersion technique followed by solution casting method where nanocellulose was prepared from micro crystalline cellulose (MCC).[13] Kashiwagi *et al.*[14] studied the thermal decomposition kinetics of PMMA in nitrogen and air atmosphere. Krul *et al.*[15] identified the MMA-MAA copolymer composition by using thermal degradation of the copolymers. Costache *et al.*[16] examined the effect of clay and carbon nanotubes on the morphologies of the PMMA/clay or PMAA/carbon nanotube nanocomposites and also investigated the degradation pathway of PMMA.

Comparative Study of the Present Results with the Previously Reported Results

Mabrouk *et al.*[12] prepared nanocomposite film via miniemulsion polymerization using acrylate latex and cellulose nanowhiskers. Polymer molecules were functionalized with methacryloxypropyl triethoxysilane (MPS) for better dispersion of the cellulose nanowhiskers into the polymer matrix. The T_g value was found to be independent of the filler content and no significant change in glass transition temperature was observed in presence of methacryloxypropyl triethoxysilane. DMA result showed a noticeable enhancement of storage modulus in presence of cellulose whiskers and reinforcing effect of cellulose whiskers was highly influenced by the MPS content above 3 wt % filler loading. Liu *et al.*[13] fabricated cellulose nanocrystals from microcrystalline cellulose via acid hydrolysis and high pressure homogenization technique and reinforced these cellulose nanocrystals in PMMA matrix by solution casting method. The nanocomposite began to degrade at slightly lower temperature than pure PMMA, but the decomposition peak increased 5–15°C over pure PMMA. Incorporation of 10 wt % cellulose nanocrystals improved the storage modulus from 1.5 GPa for pure PMMA to 5 GPa for the nanocomposite sheet. Iwata *et al.*[17] prepared PMMA/cellulose nanocomposites by immersion precipitation method using water and methanol as the nonsolvents. The thermal stability increased from 330°C for pure PMMA to 371°C for the nanocomposite with 3 wt % cellulose nanofiber loading when water was used as nonsolvent and from 333°C for pure PMMA to 351°C for the nanocomposite when methanol was used as the nonsolvent. Tensile strength of the nanocomposite with 3 wt % cellulose content increased from 34.6 to 38.6 MPa and tensile modulus increased from 761.6 to 843.2 MPa. Dong *et al.*[18] prepared uniform PMMA fibers reinforced with cellulose nanocrystals (0–41% loading). The glass transition temperature of PMMA increased from 119°C to 123–127°C and thermal stability of the PMMA/cellulose electrospun fibers also increased with increasing cellulose content. Nanoindentation study showed that storage modulus from nano-DMA measurement increased by 17% with 17 wt % cellulose nanocrystal loading. Nishioka *et al.*[19] grafted MMA onto cellulose using dimethyl sulfoxide (DMSO)/ paraformaldehyde solvent system. The grafted products were added to cellulose/PMMA blends as compatibilizers. The blends with higher grafted cellulose content showed lower thermal stability by more than 100°C than the blend without grafted product.

In comparison to the thermal stability and mechanical properties of the PMMA/cellulose blends and composites reported in earlier works, use of the surface treated CNF with MMA in case of *in situ* polymerized PMMA composite significantly enhanced the thermal stability and the glass transition temperature of the composites from 107 to 126°C. Surface treated CNF also helped to improve the tensile modulus and tensile strength by 39 and 15%, respectively than the pure polymer. Another important observation was the reduction in moisture absorption behavior of the *in situ* composites (52% lower than *ex situ* composites).

In our previous work Sain *et al.*[20] cellulose nanoparticles were prepared from jute fiber by acid hydrolysis followed by high speed homogenization and PMMA/cellulose nanocomposites were prepared by *in situ* suspension polymerization method. The experimental results suggested that a surface modification of cellulose nanoparticles is required to enhance their dispersion behavior in more hydrophobic PMMA matrix and to attain significantly improved nanocomposite properties. In this work, CNFs were surface treated with MMA to increase their dispersibility in the PMMA matrix. PMMA/MCNF composite was prepared by *in situ* suspension polymerization technique. The surface treatment of cellulose was investigated by FTIR and NMR spectroscopy. The structural and thermal properties of the composites were investigated by XRD, DSC, and TGA. Moisture absorption and tensile properties of the composite films were also measured.

EXPERIMENTAL

Materials

Raw jute fiber was obtained from local market. MMA monomer, used in this study, was procured from Merck, Germany. Benzoyl peroxide (BPO), polyvinyl alcohol (PVOH), sodium chlorite and sodium bisulfite (used for delignification step) were supplied by Loba Chemie, Mumbai. Cellulose micro and nano fibers were prepared by chemical treatment of raw jute fibers with 0.7% sodium chlorite ($NaClO_2$) solution and then with 17.5% NaOH solution to remove the lignin and hemicelluloses fractions from jute, followed by acid hydrolysis and high speed homogenization as described in our previous work.[20] Sodium hydroxide (NaOH) obtained from Merck, was used for removal of hemicelluloses fraction. The sulfuric acid used for acid hydrolysis was obtained from Merck. Acetone and chloroform (Merck) were used as solvent. Hydroquinone was

procured from Sigma–Aldrich. A high speed homogenizer (Remi High Speed Homogenizer Model No. RQ 127A) was used to reduce the cellulose particle size.

Surface Treatment of Cellulose Fibers with Methyl Methacrylate

CNFs were surface treated with MMA. The CNFs were immersed in MMA (1 : 7 w/v) under constant stirring at 50°C for 2 h. Hydroquinone was added in order to minimize the effect of free radical reaction at the unsaturated end of the MMA molecules.[5] Surface treated fibers (MCNFs) were then separated by filtration and dried at room temperature and then under vacuum at 60°C.

Preparation of PMMA/MCNF Nanocomposite

Surface treated cellulose micro/nanofibers (MCNFs), 10% w/w with respect to the monomer MMA (matrix phase) were dispersed in the deionized water. PVOH (6% w/v with respect to the monomer) was added to stabilize the suspension, and the mixture was heated to 85°C with constant stirring. Benzoyl peroxide (3% w/w with respect to the monomer) was added to the monomer MMA and this mixture was slowly added to the suspension medium in the reactor. The polymerization reaction was carried out at 85°C for 4 h and then at 90°C for 1 h with continuous stirring. PMMA/MCNF composite granules were formed in the suspension medium (designated as MMIPC). The composite granules were filtered and washed with hot water several times to remove any PVOH adhered to the granules. The composite granules were then dried under vacuum at 80°C overnight and then films were prepared by solution casting method after sonicating the MMIPC dispersion in chloroform for 3 h. The thickness of the MMIPC films was 135 μm. Pure PMMA without any filler was also prepared by the similar suspension polymerization technique. PMMA films were prepared by solution casting method and the thickness of the film was 138 μm. PMMA/MCNF composites were also prepared by conventional *ex situ* dispersion technique. The suspension polymerized PMMA granules were first dissolved in chloroform and then 10 wt % (w/w with respect to PMMA) MCNF were dispersed in the PMMA solution by sonication for 3 h. Films were then prepared by solution casting method designated as MMEPC and the thickness of the film was 132 μm.

Characterization Techniques of MCNF and PMMA/MCNF Composites

Average diameter of the extracted CNFs was measured with Malvern V2.0 (Malvern Instruments) and it was in 350 nm range.

The MCNF, CNF powders and PMMA composite film samples were subjected to FTIR analysis with Perkin–Elmer Infrared Spectrophotometer (Spectrum 100) in the spectral range of 4000–400 cm^{-1}, using the KBr pellet method.

^{1}H-nuclear magnetic resonance (^{1}H-NMR) spectra of modified and unmodified CNF were recorded on a NMR spectrometer (Bruker, DRX 400 MHz). DMSO-*d6* was used as a solvent and tetramethylsilane (TMS) as reference.

In situ PMMA/MCNF composite film was first dissolved in tetrahydrofuran (THF), and then filtered to separate the MCNF. Then methyl alcohol, which is a nonsolvent for PMMA, was added to the filtrate with stirring to reprecipitate the polymer. The reprecipitated PMMA was further filtered and collected and dried under vacuum at 80°C. Then viscosity average molecular weight of the unreinforced PMMA and the PMMA extracted from the *in situ* polymerized PMMA/MCNF composites were determined by the viscometric method in chloroform following the Mark–Houwink equation: $[\eta] = KM_v^a$, where $[\eta]$ is the intrinsic viscosity of the solution, $K = 0.34 \times 10^4$ and $a = 0.83$ at 25°C for chloroform. The unit of Mark–Houwink intercept is inverse concentration, that is, dL g^{-1}.

Surface morphology of the PMMA and PMMA/MCNF composite powder was investigated with Scanning electron microscope (HITACHI-S-3400N) with a gold coating operating at 5 kV.

The size of CNF and the extent of dispersion of MCNF in the PMMA matrix in MMIPC was examined under Transmission electron microscope (HRTEM: JEOL JEM 2010) operating at an accelerating voltage of 200 kV.

X-ray diffraction (XRD) was conducted utilizing X-ray diffractometer, (X'Pert PRO) Model RIGAKU MINISLEX employing Cu Kα radiation ($k = 0.154$ nm) with a power of 40 kV $\times$ 35 mA and a scan rate of 2° min^{-1}.The diffraction angle (2θ) ranged from 5° to 60°.

Differential scanning calorimetric (DSC) analysis was performed done using a DSC (DSC Q20 V24.4 Build 116, TA Instruments) with a temperature ramp from 30 to 210°C at a heating rate of 10°C min^{-1} under nitrogen atmosphere.

Thermogravimetric analysis (TGA) was done using a Mettler-Toledo TGA/SDTA851e from 25 to 600°C at a heating rate of 10°C min^{-1} under nitrogen atmosphere.

Tensile tests were performed on the solution cast films using a Lloyd Universal Testing Machine according to ASTM D638 method. Five measurements were conducted for each sample, and the results were averaged to obtain a mean value.

The composite samples were subjected to moisture absorption test. The test was carried out by taking films of dimensions of approximately (10 $\times$ 10 $\times$ 0.20 mm^3). The films were dried, weighed, and conditioned at room temperature in a dessicator containing a saturated solution of KNO_3 to ensure 93% RH. The samples were weighed at desired time intervals until an equilibrium weight was reached. The moisture uptake (% MU) of each sample was calculated following: % MU = $\{(M_t - M_0)/M_0\} \times 100$, where, M_t and M_0 are the weight of the sample at time "t" in 93% relative humidity (RH) and the initial weight of the sample before exposure to 93% RH, respectively. Five measurements were taken for each sample, and the results were averaged to obtain a mean value.

RESULTS AND DISCUSSION

Characterizations of MMA Treated Cellulose Micro/Nano Fibers (MCNF)

To confirm the surface treatment of CNF, MCNF was subjected to FTIR and ^{1}H NMR spectroscopy (Figures 1 and 2, respectively). FTIR Spectra of CNF and MCNF are presented in Figure 1. Unmodified CNF showed characteristic peaks of

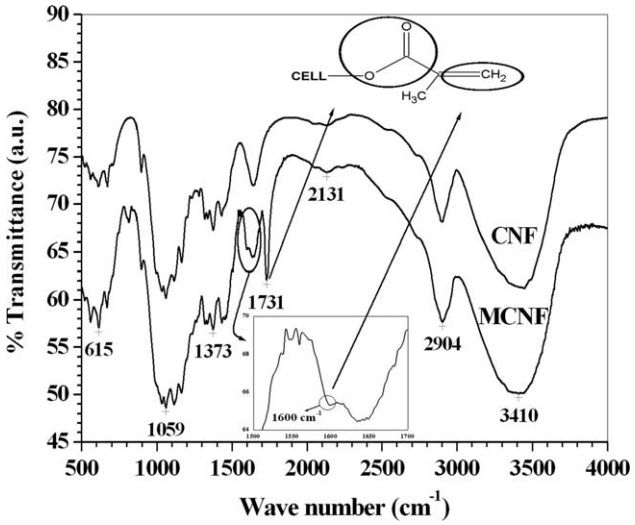

Figure 1. FTIR plots of CNF and MCNF.

hydrogen-bonded —OH stretching at 3410 cm^{-1}, the —OH bending of the adsorbed water at 1643 cm^{-1}, the C—H stretching at 2904 cm^{-1}, the C—H and C—OH in-plane bending vibrations at 1432 cm^{-1}, the C—H deformation vibration at 1373 cm^{-1}.[21] While in case of MCNF spectra, along with the above mentioned characteristic peaks of cellulose, there were

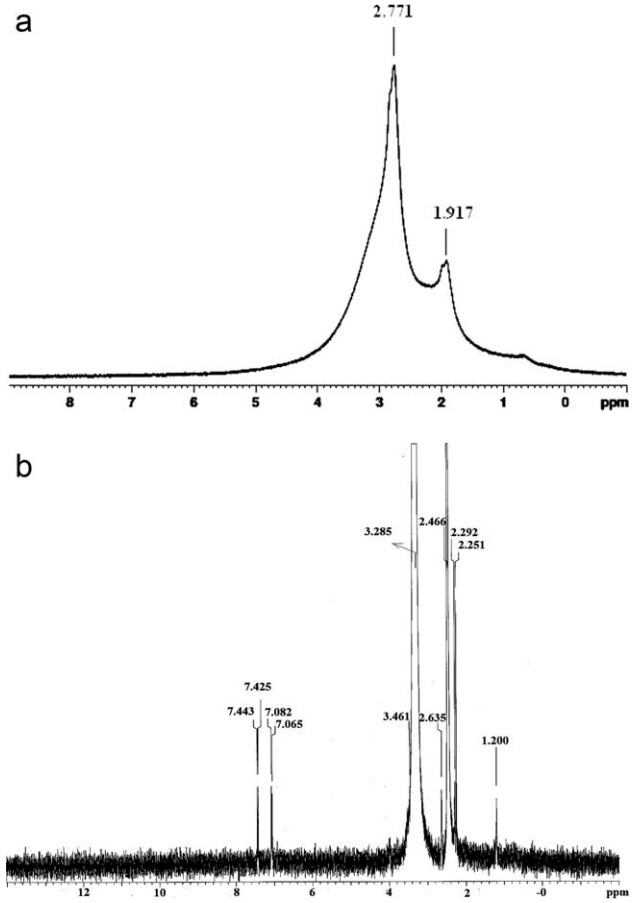

Figure 2. ^{1}HNMR plots of (a) CNF, (b) MCNF.

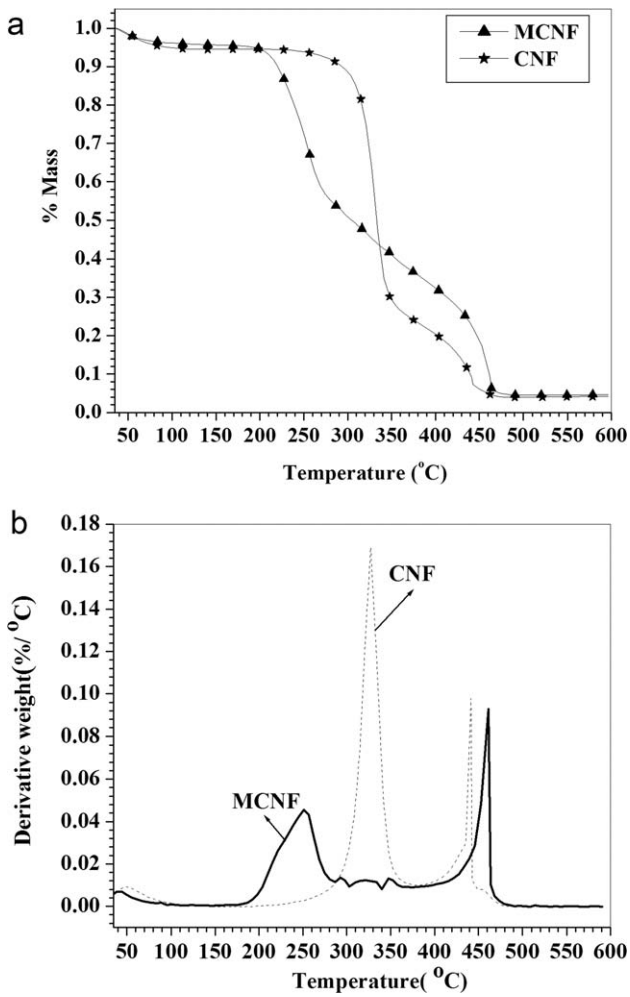

Figure 3. (a) TGA and (b) DTGA plots of MCNF and CNF.

distinct characteristic sharp peak of ester carbonyl at 1731 cm^{-1} along with C═C double bond peak at 1600 cm^{-1} (inset, Figure 1) clearly indicating the presence of —O—C═O bonds.[3] A small but sharp peak was also evident at 820 cm^{-1} corresponding to methylene rocking mode vibration which was absent in untreated CNF. The broadness of H-bonded —OH stretching indicated that the modification yield might be small. The unsaturation present on the surface of MCNF was likely to take part in free radical polymerization with MMA imparting a strong interface in MMIPC. Figure 2(a,b) represents ^{1}H NMR spectra of unmodified CNF and MCNF, respectively. For MCNF, peaks at $\delta = 3.285–3.461$ corresponded to protons of ester methylene group, and other sharp signals confirmed relative increase of proton signals of MMA while untreated CNF showed only two broad peaks at $\delta = 1.917$ and $\delta = 2.771$ corresponding to two types of hydrogens present in the cellulose.

Thermal Analysis of CNF and MCNF

TGA was carried out to investigate the thermal stability of the MCNF in comparison to that of the CNF, shown in Figure 3. The decomposition of cellulose occurred in three stages. The first stage of weight loss was due to the loss of moisture while

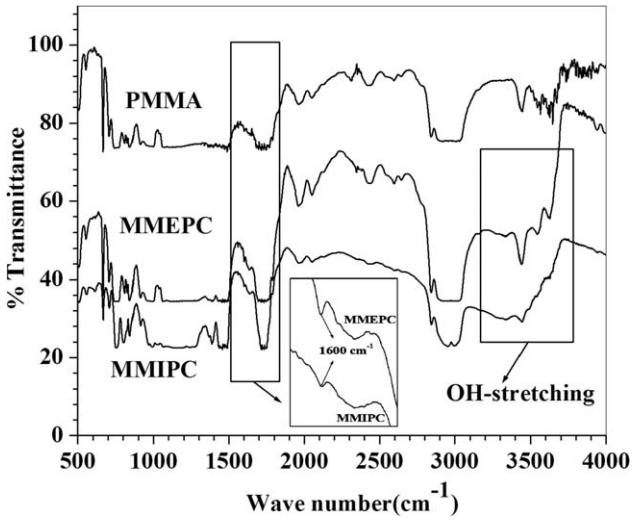

Figure 4. FTIR plots of PMMA, MMIPC, and MMEPC.

others were attributed to the pyrolysis.[22] The first degradation temperature of MCNF shifted to a lower temperature (251°C) compared to that of the untreated ones (326°C). But the final degradation of MCNF was delayed and the peak appeared at a higher temperature of 461°C compared to that of the CNF (441°C) showing higher thermal stability of MCNF. The final decomposition temperature of the MMA treated cellulose fibers was delayed indicating increased bulking and OH group modification to give good dimensional stability.[23] CNF showed a degradation peak at 440–450°C range which corresponded to the decomposition of lignin fraction.[24] This indicates the presence of trace amount of lignin which was not completely removed during the chemical treatment of jute fibers. However, the amount of lignin present in the sample was negligible as 99.94% weight loss had already occurred before reaching this temperature.

Characterizations of PMMA/MCNF Composite (MMIPC)

Molecular Weight. The viscosity average molecular weights (M_V) of the unreinforced PMMA and PMMA extracted from MMIPC film were determined by viscometric method. The M_v of PMMA extracted from the MMIPC film was 74,300 g mol^{-1}, whereas for unreinforced PMMA, it was 56,700 g mol^{-1}, indicating a 31% increase in the molecular weight. This might be due to the increase in the length of the propagating radicals before they could find one another and terminate due to the hindrance caused in their movement in space by the presence of the MCNF. A similar observation was also reported earlier.[25]

FTIR Study. PMMA/MCNF composites (MMIPC and MMEPC) were subjected to FTIR analysis (Figure 4) to investigate the bonding between PMMA and cellulose in MMIPC and MMEPC. PMMA showed characteristic peaks of methylene C—H stretching vibrations ranging from 2900 to 3050 cm^{-1}, the C═O stretching mode (1724 cm^{-1}), C—O stretching (1444 cm^{-1}), C—H stretching symmetric and asymmetric mode (1393 cm^{-1}) and the α-methyl group (994 cm^{-1}). While in MMIPC, a small but distinct hump appeared in the range of 3080 cm^{-1} to 3380 cm^{-1}, which are characteristic, absorptions of the free —OH and the H-bonded —OH groups of cellulose, confirming the presence of MCNF. The C═C— bond peak intensity at 1600 cm^{-1} decreased significantly (inset Figure 4) in MMIPC indicating their participation in the polymerization along with MMA, while in *ex situ* composites (MMEPC), the —C═C— peak was more predominant as they remained unchanged during the *ex situ* dispersion process.

Structure and Morphology of the Composites. The incorporation and attachment of MCNF within the PMMA molecules in the MMIPC composite granules was observed via scanning electron microscope (SEM), shown in Figure 5. The unreinforced PMMA appeared like pearl beads of various sizes ranging between 10 and 40 μm diameters with more or less smooth surfaces [Figure 5(a)]. The MMIPC granules were slightly lower in diameter than that of neat PMMA beads with surfaces covered with MCNF particles [Figure 5(b)].

The size and shape of CNF was investigated under TEM [Figure 6(a)]. MMIPC granules, when dissolved in chloroform, highly diluted and examined under TEM [Figure 6(b)], revealed the

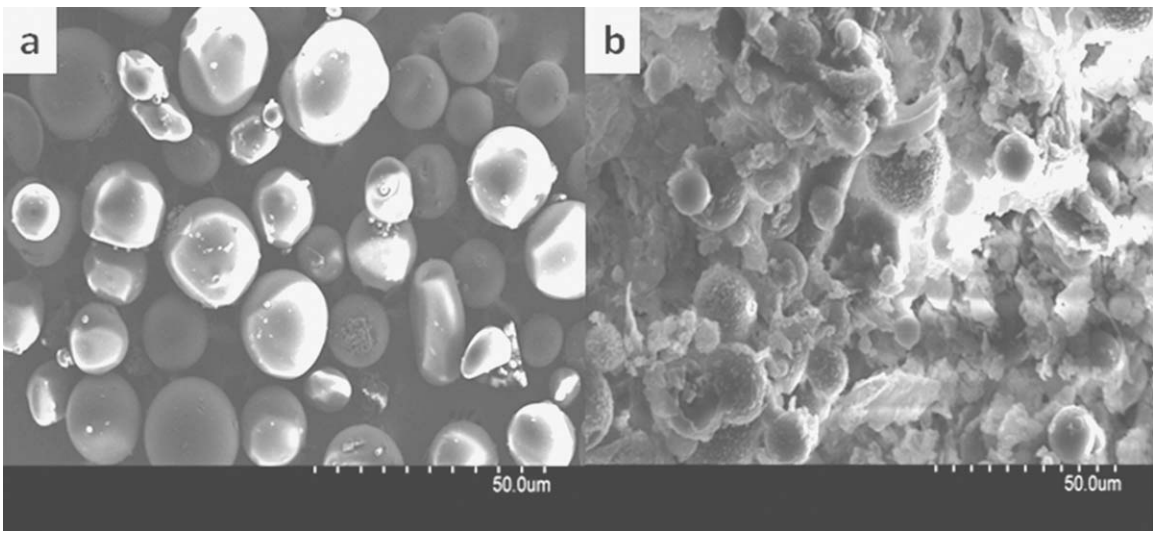

Figure 5. SEM pictures of (a) PMMA (b) MMIPC (Maginification; 1.00K).

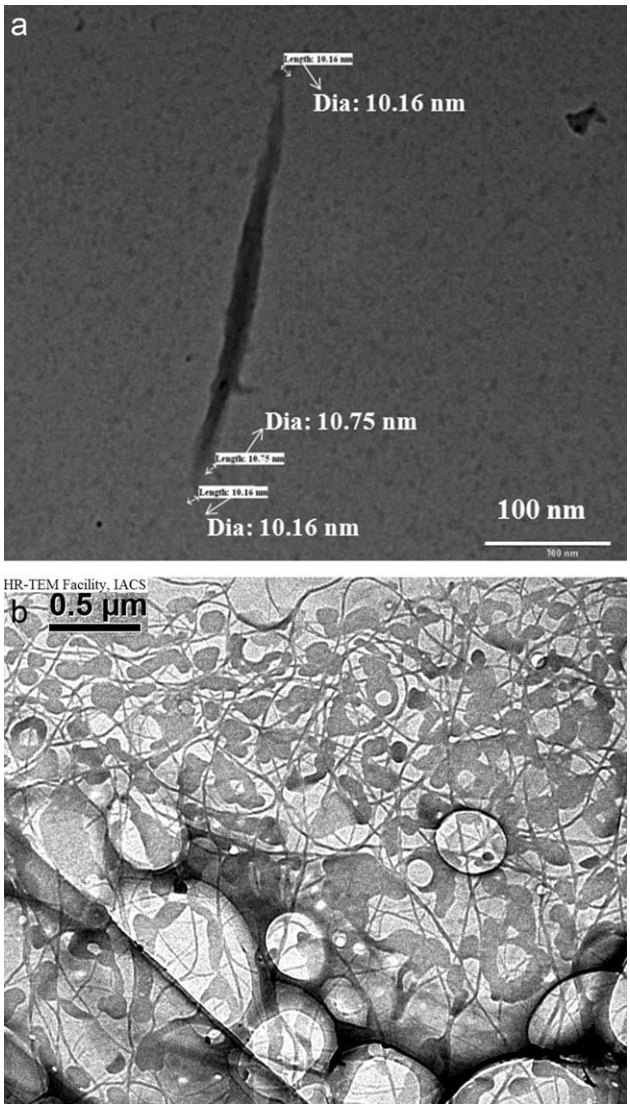

Figure 6. TEM pictures of (a) CNF and (b) MMIPC.

attachment of the MCNF with the polymer matrix and a fibrillar network of MCNF was also evident.[26]

CNF and MCNF showed characteristic peaks at 2θ of 12.1°, 14.8°, 16.64°, 20.1°, 22.45°, and 34.43°. The peak at 2θ of 14.8°, 16.64°, 22.45°, and 34.43° corresponded to the plane (101), (101), (002), and (040) respectively[27] shown in Figure 7. These are the characteristic peaks of cellulose I, whereas the peaks at 2θ of 12.1°, 20.1°, and 34.43° corresponded to the plane (101), (101), and (040), are the characteristic peaks of cellulose II. It is seen that the both cellulose I and II are present in the extracted cellulose fiber from jute. Surface treatment of CNF occurred successfully, as shown previously in the FTIR and NMR results, but it did not change the cellulose structure. X-ray diffraction spectra of PMMA, MMIPC, and MMEPC are shown in Figure 8. The presence of small but a sharp peak at $2\theta = 22.3°$ (002 plane) in MMEPC confirmed the presence of cellulose I in the films. In MMIPC an additional peak was observed at $2\theta = 20°$ which can be attributed to the (101) plane of cellulose II.[28]

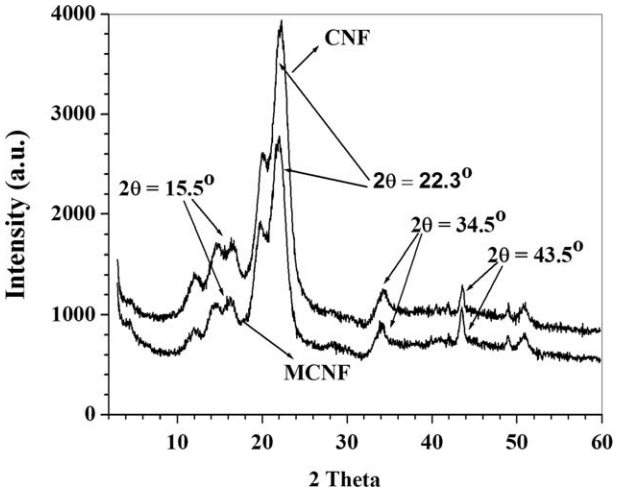

Figure 7. XRD plots of CNF and MCNF.

Mechanical Properties of Composites. Tensile strength, Young's modulus and stress/strain plots of PMMA/MCNF composites are shown in Figure 9. Both tensile strength [Figure 9(a)] and Young's modulus [Figure 9(b)] of MMIPC improved significantly indicating increased stress transfer at the interface. A homogeneous dispersion and an improved interfacial interaction of MCNF with the PMMA molecules in MMIPC might be responsible for such improvement in properties. The tensile strength and Young's modulus improved by 15 and 39%, respectively in MMIPC which might be due to the formation of a network structure[17] as observed from TEM (Figure 6). Both the values decreased in MMEPC compared to that of the unreinforced PMMA. In MMEPC, the dispersion of MCNF was nonuniform and only H-bonding could have occurred at the filler/matrix interface through the ester linkage of PMMA and OH groups of MCNF.

Thermal Properties of Composites. The DSC curves (Figure 10) of PMMA, MMIPC, and MMEPC films were investigated to get an insight of the structure of the composites. From the DSC curves, glass transition temperature (T_g) of neat PMMA was found to be at 107°C, whereas, in MMIPC, T_g shifted to a

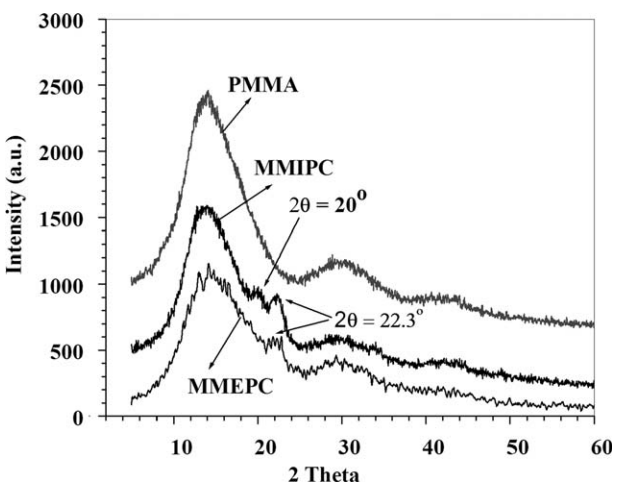

Figure 8. XRD plots of PMMA, MMIPC, and MMEPC.

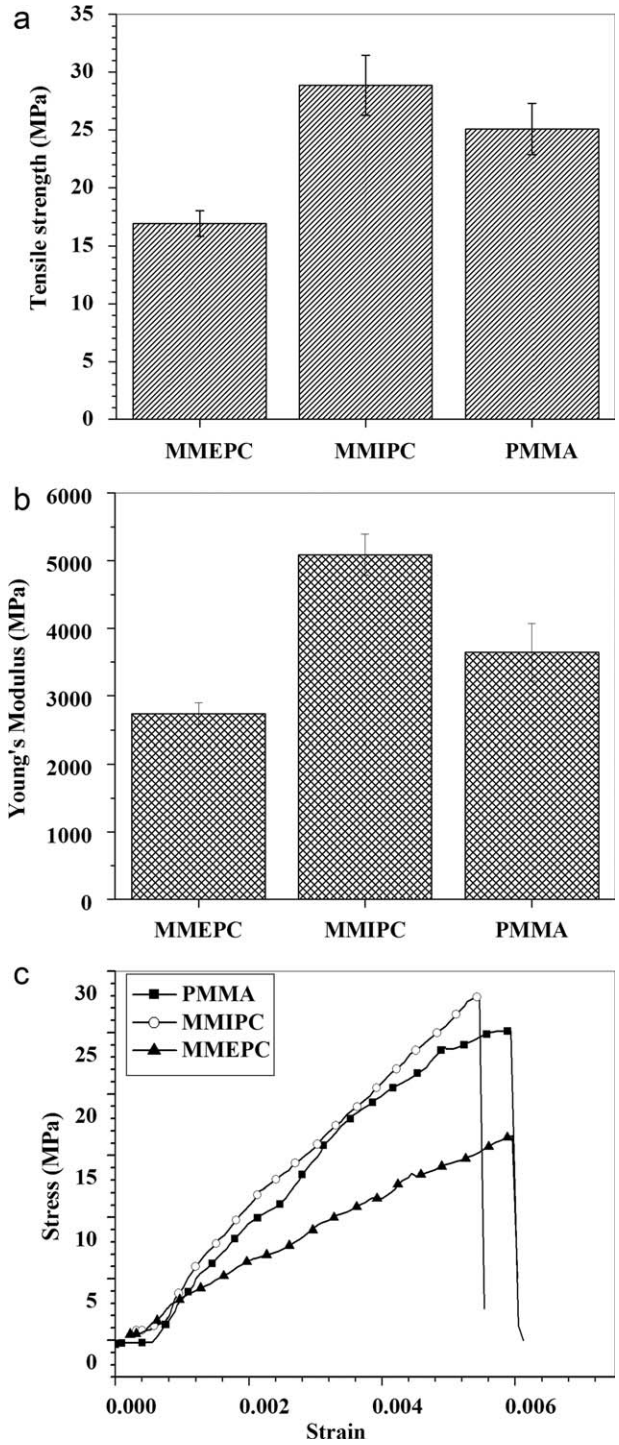

Figure 9. (a) Tensile strength of PMMA, MMIPC, and MMEPC (b) Young's modulus of PMMA, MMIPC, and MMEPC, and (c) Stress–strain plot of PMMA, MMIPC, and MMEPC.

higher temperature 126°C. The increase in T_g in MMIPC could be attributed to the restricted segmental motion of the PMMA molecules near the interface due to stronger interfacial bonding. Another factor contributing towards the increase in T_g might be an increased chain length as evident from viscosity average molecular weight determination. The T_g of MMEPC was nearly

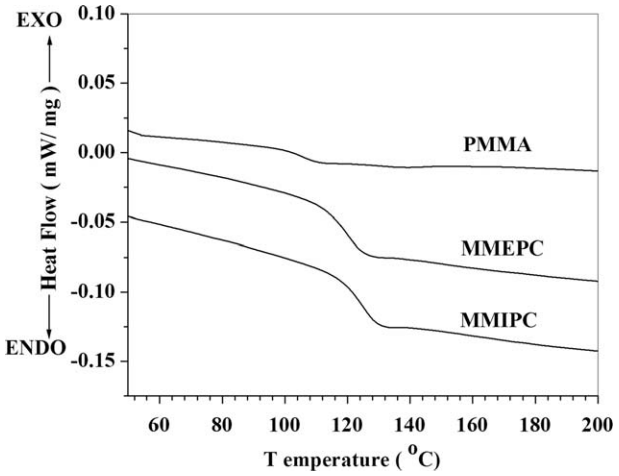

Figure 10. DSC graph of PMMA, MMIPC, and MMEPC.

119°C, which was 12°C higher than that observed for PMMA alone. This shift can be ascribed to the H-bonding between the MCNF fillers and the ester groups of PMMA molecules.

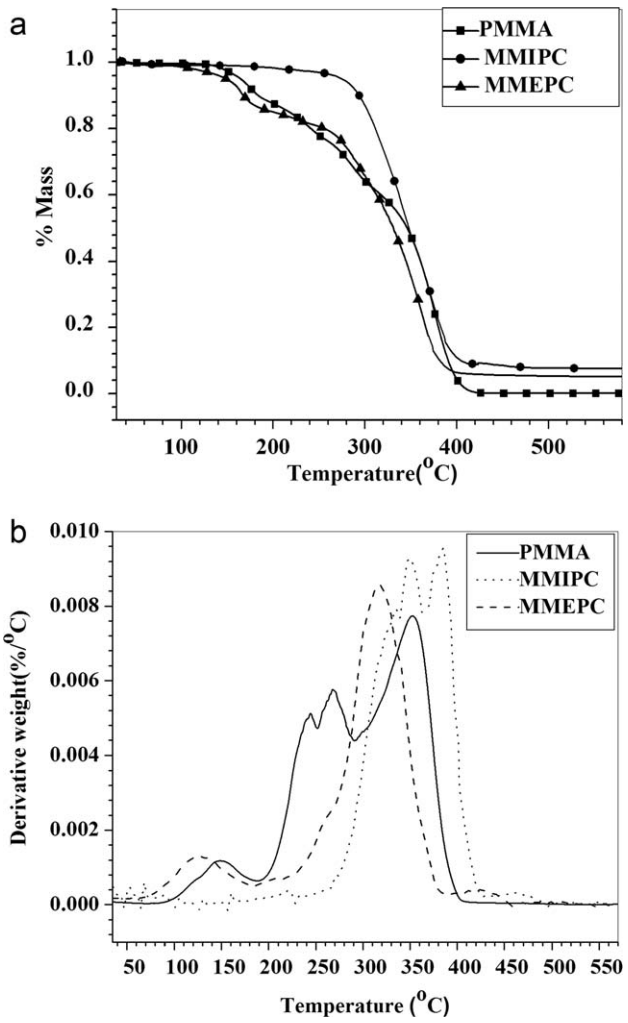

Figure 11. (a) TGA and (b) DTGA plots of PMMA, MMIPC, and MMEPC.

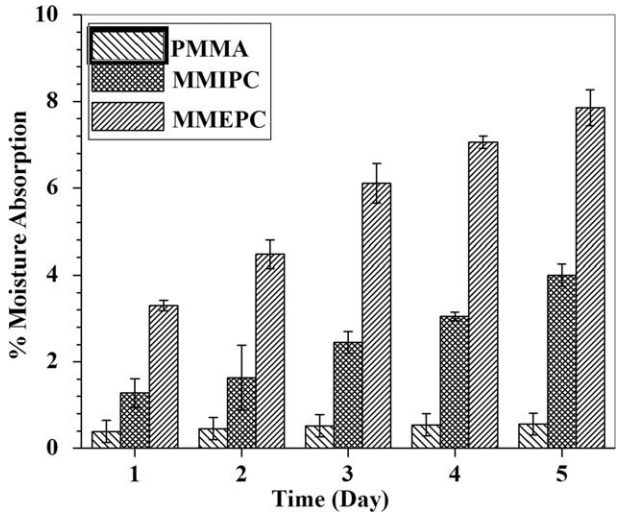

Figure 12. Moisture absorption behavior of PMMA, MMIPC, and MMEPC.

Thermal Stability. TGA and DTGA curves of unreinforced PMMA, MMIPC, and MMEPC are shown in Figure 11(a,b), respectively. Thermal decomposition of pure PMMA takes place in two steps.[12,14] The decomposition raging from 165 to 195°C corresponds to the cleavage of the carbon-carbon bonds between units linked head to head and from 270 to 300°C correspond to the cleavage of terminal vinyl units.[14] The TGA curve appeared to be a single step degradation process in MMIPC which occurred in the temperature range between 280 and 290°C. Thus the main chain degradation of the MMIPC composite was delayed by about 20–25°C than that of unreinforced PMMA and also no degradation peak appeared before that. It demonstrated that MMIPC composites had enhanced thermal stability than that of pure PMMA. The strong interaction between MCNF and the PMMA chains might have prevented the thermal degradation at a lower temperature and increased the thermal stability. In case of MMEPC graph again two step degradation was evident like neat PMMA. The first degradation was ranging between 150 and 160°C and final degradation took place at 274°C, higher than that observed for unreinforced PMMA.

Moisture Absorption Study. Cellulose is hydrophilic in nature with a strong tendency to absorb moisture. This property restricts the wide use of cellulose fibers as filler in polymer composites. The moisture uptake of MMIPC and MMEPC were measured in comparison to that of PMMA alone (Figure 12) to investigate the effect of two different fabrication processes. The % moisture uptake of MMIPC was 52% lower than that of MMEPC although both contained same amount of MCNF fillers. This was a very important observation which clearly indicated that incorporation of cellulose fillers into polymer matrix by *in situ* polymerization technique is an effective way of reducing the moisture absorption tendency of cellulosic filler reinforced composites. In MMIPC, the availability of free —OH groups was lower as the MCNF fillers were embedded within the PMMA matrix and were less exposed to the environment, which led to a significant decrease in moisture absorption. Whereas in MMEPC, the —OH groups were much more exposed to the environment and were able to absorb moisture from the atmosphere.

CONCLUSIONS

Cellulose micro/nanofibers were extracted from raw jute fibers and were surface treated with MMA. Surface treatment led to better dispersion of MCNF in PMMA matrix during *in situ* polymerization method. The possible interaction between MCNF and PMMA molecules during free radical polymerization resulted in an improved mechanical, thermal and moisture resistance property. The composites prepared by *ex situ* dispersion technique showed much lower properties. This study therefore depicted two points very clearly: First, suitable surface treatment of cellulose (with MMA here) helps in improved dispersion of such hydrophilic fillers in a hydrophobic matrix like PMMA. And second, *in situ* polymerization technique is an effective way of producing such cellulosic filler reinforced composites where improved properties can be achieved as well as engulfment of cellulosic fillers by long polymeric chains significantly reduces the moisture uptake property which can be a major advantage for various applications.

ACKNOWLEDGMENTS

Sunanda Sain is thankful to CSIR (Council of Scientific and Industrial Research), New Delhi, Government of India, for providing her fellowship.

REFERENCES

1. O'sullivan, A. C. *Cellulose* **1997**, *4*, 173.
2. Dankovich, T. A.; Hsieh, Y. L. *Cellulose* **2007**, *14*, 469.
3. Liu, H.; Hsieh, Y. L. *J. Polym. Sci. Polym. Phys.* **2003**, *41*, 953.
4. Botaro, V. R.; Gandini, A. *Cellulose* **1998**, *5*, 65.
5. Pracella, M.; Haque, M. U.; Alvarez, V. *Polymer* **2010**, *2*, 554.
6. Liu, C. F.; Zhang, A. P.; Li, W. Y.; Sun, R. C. In Ionic Liquids: Applications and Perspectives; Kokorin, A., Ed.; InTech: Croatia, **2011**; p 81.
7. Heydarzadeh, H. D.; Najafpour, G. D.; Nazari-Moghaddam, A. A. W. A. S. J. *World Appl. Sci. J.* **2009**, *6*, 564.
8. George, J.; Sreekala, M. S.; Thomas, S. A. *Polym. Eng. Sci.* **2001**, *41*, 1471.
9. Huang, X.; Brittain, W. *J. Macromolecules* **2001**, *34*, 3255.
10. Meneghetti, P.; Qutubuddin, S. *Langmuir* **2004**, *20*, 3424.
11. Meneghetti, P.; Qutubuddin, S. *Thermochim. Acta.* **2006**, *442*, 74.
12. Mabrouk, A. B.; Kaddami, H.; Magnin, A.; Belgacem, M. N.; Dufresne, A.; Boufi, S. *Polym. Eng. Sci.* **2011**, *51*, 62.
13. Liu, H.; Liu, D.; Yao, F.; Qinglin, W. *Bioresource Technol.* **2010**, *101*, 5685.
14. Kashiwagi, T.; Inaba, A.; Brown, J. E.; Hatada, K.; Kitayama, T.; Masuda, E. *Macromolecules* **1986**, *19*, 2160.
15. Krul, L. P.; Yakimtsova, L. B.; Egorova, E. L.; Matusevich, Y. I.; Selevich, K. A.; Kurtikova, A. L. *Russ. J. Appl. Chem.* **2009**, *82*, 1636.

16. Costache, M. C.; Wang, D.; Heidecker, M. J.; Manias, E.; Wilkie, C. A. *Polym. Adv. Technol.* **2006**, *17*, 272.
17. Fahma, F.; Hori, N.; Iwata, T.; Takemura, A. *J. Appl. Polym. Sci.* **2013**, *128*, 1563.
18. Dong, H.; Strawhecker, K. E.; Snyder, J. F.; Orlicki, J. A.; Reiner, R. S.; Rudie, A. W. *Carbohydr. Polym.* **2012**, *87*, 2488.
19. Nishioka, N.; Yamaoka, M.; Haneda, H.; Kawakami, K.; Uno, M. *Macromolecules* **1993**, *26*, 4694.
20. Sain, S.; Ray, D.; Mukhopadhyay, A.; Sengupta, S.; Kar, T.; Ennis, C. J.; Rahman, P. K. S. M. *J. Appl. Polym. Sci.* **2012**, *126*, E127.
21. Nadanathangam, V.; Satyamurthy, P. In Proceedings of IPCBEE-7 Conference; Singapore, **2011**; 181.
22. Melo, J. C. P. D.; Filho, S. E. C. D.; Santana, S. A. A.; Airoldi, C. *Colloid Surface A.* **2009**, *346*, 138.
23. Sonowal, J.; Gogoi, P. K. *IJC* **2010**, *2*, 218.
24. Van Le, S. L. In Concise Encyclopedia of Wood and Wood Based Materials: Thermal Properties; Schniewind, A. P., Ed.; Pergamon Press: Elmsford, NY, **1989**; p 271.
25. Nikolaidis, A. K.; Achilias, D. S.; Karayannidis, G. P. *Ind. Eng. Chem. Res.* **2011**, *50*, 571.
26. Zimmermann, T.; Pöhler, E.; Geiger, T.; Schleuniger, J.; Schwaller, P.; Richter, K.; Eds. ACS Symposium Series 938; American Chemical Society: Washington, DC, **2006**; p 33.
27. Ford, E. N. J.; Mendon, S. K.; Thames, S. F.; Rawlins, J. W. *J. Eng. Fiber. Fabr.* **2010**, *5*, 10.
28. Lu, P.; Hsieh, Y. L. *Nanotechnology* **2009**, *20*, 415604.